

LANGMUIR

Subscriber access provided by Kaohsiung Medical University

Interfaces: Adsorption, Reactions, Films, Forces, Measurement Techniques, Charge Transfer, Electrochemistry, Electrocatalysis, Energy Production and Storage

Electrostatically Driven Protein Adsorption: Charge Patches versus Charge Regulation

Fernando M. Boubeta, Galo J A A Soler-Illia, and Mario Tagliacruz

Langmuir, **Just Accepted Manuscript** • DOI: 10.1021/acs.langmuir.8b03411 • Publication Date (Web): 19 Nov 2018Downloaded from <http://pubs.acs.org> on November 20, 2018

Just Accepted

“Just Accepted” manuscripts have been peer-reviewed and accepted for publication. They are posted online prior to technical editing, formatting for publication and author proofing. The American Chemical Society provides “Just Accepted” as a service to the research community to expedite the dissemination of scientific material as soon as possible after acceptance. “Just Accepted” manuscripts appear in full in PDF format accompanied by an HTML abstract. “Just Accepted” manuscripts have been fully peer reviewed, but should not be considered the official version of record. They are citable by the Digital Object Identifier (DOI®). “Just Accepted” is an optional service offered to authors. Therefore, the “Just Accepted” Web site may not include all articles that will be published in the journal. After a manuscript is technically edited and formatted, it will be removed from the “Just Accepted” Web site and published as an ASAP article. Note that technical editing may introduce minor changes to the manuscript text and/or graphics which could affect content, and all legal disclaimers and ethical guidelines that apply to the journal pertain. ACS cannot be held responsible for errors or consequences arising from the use of information contained in these “Just Accepted” manuscripts.

**ACS Publications**is published by the American Chemical Society, 1155 Sixteenth Street N.W.,
Washington, DC 20036Published by American Chemical Society. Copyright © American Chemical Society.
However, no copyright claim is made to original U.S. Government works, or works
produced by employees of any Commonwealth realm Crown government in the course
of their duties.

Electrostatically Driven Protein Adsorption: Charge Patches versus Charge Regulation

F. M. Boubeta¹, G. J. A. A. Soler-Illia^{2,3}, M. Tagliazucchi^{1,2,}*

1. INQUIMAE, Facultad de Ciencias Exactas y Naturales, Universidad de Buenos Aires, Ciudad Universitaria, Pab. II, C1428EHA, Ciudad Autónoma de Buenos Aires, Argentina

2. DQIAQF, Facultad de Ciencias Exactas y Naturales, Universidad de Buenos Aires, Ciudad Universitaria, Pab. II, C1428EHA, Ciudad Autónoma de Buenos Aires, Argentina.

3. Instituto de Nanosistemas, Universidad Nacional de General San Martín, Av. 25 de Mayo y Francia, 1650, San Martín, Argentina.

ABSTRACT

The mechanisms of electrostatically driven adsorption of proteins on charged surfaces are studied with a new theoretical framework. The acid-base behavior, charge distribution and electrostatic contributions to the thermodynamic properties of the proteins are modeled in the presence of a charged surface. The method is validated against experimental titration curves and apparent pK_as. The theory predicts that electrostatic interactions favor the adsorption of proteins at their isoelectric points on charged surfaces despite the fact that the protein has no net charge in solution. Two known mechanisms explain adsorption under these conditions: i. charge regulation (the charge of the protein changes due to the presence of the surface) and ii. charge patches (the protein orients to place charged

1
2
3 amino acids near opposite surface charges). This work shows that both mechanisms contribute to
4 adsorption at low ionic strengths, while only the charge-patches mechanism operates at high ionic
5 strength. Interestingly, the contribution of charge regulation is insensitive to protein orientation under
6 all conditions, which validates the use of constant-charge simulations to determine the most stable
7 orientation of adsorbed proteins. The present study also shows that the charged surface can induce
8 large shifts in the apparent pKas of individual aminoacids in adsorbed proteins. Our conclusions are
9 valid for all proteins studied in this work (lysozyme, α -amylase, RNase and β -lactoglobuline), as
10 well as for proteins that are not isoelectric, but have instead a net charge in solution of the same sign
11 as the surface charge, i.e. the problem of protein adsorption on the ‘wrong side’ of the isoelectric
12 point.
13
14
15
16
17
18
19
20
21
22
23
24
25

26 **Introduction**

27
28 Protein adsorption on charged surfaces is a technologically relevant phenomena¹⁻³ and a very active
29 area of fundamental research.^{4,5} During adsorption, proteins interact with the substrate through a
30 combination of electrostatic, van der Waals, hydrogen-bond and hydrophobic interactions.^{4,6} On
31 highly charged substrates, electrostatic interactions will be a dominant force and the amount of
32 adsorbed protein will depend on the net charge of the protein. Intuitively, it may be expected that a
33 requisite for electrostatically driven adsorption is that the protein and the surface should have charges
34 of opposite sign. However, various experiments have shown that protein adsorption can occur on bare
35 or polyelectrolyte-modified surfaces even when the charges of the protein and the surface are of the
36 same sign.⁷⁻¹² Furthermore, in many reports, protein adsorption displays a maximum at pHs near the
37 isoelectric point (IEP) of the protein.^{10,13,14} In principle, these observations can be ascribed to the role
38 of non-electrostatics forces, which will lead to protein adsorption even in the presence of unfavorable
39 electrostatic interactions. However, such conclusion fails to explain many experiments where the
40
41
42
43
44
45
46
47
48
49
50
51
52
53
54
55
56
57
58
59
60

1
2
3 amount of adsorbed protein decreases with increasing ionic strength.^{7,10,11,15-17} Such dependence of
4 adsorption with ionic strength suggests that electrostatic interactions favor adsorption even for
5 proteins with zero net charge or proteins with a charge of the same sign as that of the surface. Two
6 mechanisms have been proposed to explain this result, the charge-regulation (CR) effect¹⁸⁻²⁰ and the
7 charge-patches (CP) mechanism.^{15,16,21} In the CR effect, the presence of the charged surface induces
8 a charge of the opposite sign in the protein by displacing the acid-base chemical equilibria of its
9 aminoacids, thus favoring adsorption. The CP mechanism is based on the presence of “charge
10 patches” in the protein, which are defined as regions on the protein surface that have an elevated
11 content of aminoacids of the same charge. These charge patches allow a favorable protein-surface
12 interaction for protein orientations that place patches with a charge opposite to the surface near it and
13 patches with the same charge as the surface, far from it. The charge patches are thus related to the
14 charge distribution of the protein, whose first moment, the electric dipole of the protein, has been
15 used in the past to explain protein orientation on charged surfaces.²²

16
17
18
19
20
21
22
23
24
25
26
27
28
29
30
31
32
33 The CR effect has been predicted theoretically^{23,24} and confirmed experimentally²⁵⁻²⁷ in different
34 systems and it is partially responsible for the fact that the pKa of a free aminoacid in solution can be
35 very different from the pKa of the same aminoacid inside a protein.^{28,29} In other words, the protonation
36 state of an acid or basic group depends not only on the pH of the solution but also on the local
37 chemical environment, including the presence of neighbor charged groups and the local dielectric
38 properties.^{23,30} These interactions will affect the acid-base equilibrium of an aminoacid compared to
39 a bulk solution and will lead to an apparent pKa (*i.e.* the pKa of the aminoacid inside the protein)
40 different from the pKa of the same aminoacid free in solution. Placing the protein near a highly
41 charged interface will further modify the pKa value of that aminoacid, which now will be influenced
42
43
44
45
46
47
48
49
50
51
52
53
54
55
56
57
58
59
60

1
2
3 by both the charge of the surface and the charges of neighboring aminoacids (which will also be
4 affected by the presence of the surface).^{18,19}
5
6

7
8 The adsorption of proteins on surfaces of the same charge has been studied by both theory and
9 simulation in the past. For example, atomistic molecular dynamics (MD) simulations have been used
10 to study the adsorption of negatively charged BSA on a negative surface.³¹ However that study, as
11 well as most MD studies of proteins, fixed the charge of the aminoacids, thus neglecting the CR
12 effect. Constant-pH MD simulations^{32,33} include the CR effect, but, to the best of our knowledge, they
13 have not been used to study how CR affects protein adsorption. Moreover, the estimation of
14 adsorption free energies is still very difficult for both constant-charge and constant-pH MD
15 simulations due to the difficulty of statistical sampling the free energy landscape.⁶
16
17
18
19
20
21
22
23
24
25

26 The CR mechanism for a protein in solution can be predicted and studied with different theoretical
27 methods, including those based on the Poisson-Boltzmann equation (for example, DelPhi³⁴ and
28 Fambe-pH,³⁵ among others), electrostatics-conformational methods (*e.g.* MCCE³⁶) and empirical
29 methods (*e.g.* propKa³⁷). The available implementations of these methodologies do not allow to
30 straightforwardly include a charged surface in the calculations, which is possible with the theoretical
31 framework introduced in this work. The relative importance of the CR and the CP mechanisms for
32 the adsorption of proteins on surfaces of the same charge have also been the subject of previous
33 theoretical investigations. For example, de Vos *et al.* studied the CR and CP mechanisms for brush-
34 modified surfaces using an asymmetrically charged cylinder and concluded that CR is more important
35 than CP at low ionic strengths.³⁸ Longo and Szleifer studied protein adsorption into polyelectrolyte
36 gels using a molecular theory that allowed inhomogeneities in one spatial direction and also identified
37 CR as the dominant mechanism.¹⁹ It is worthwhile to note that these previous theoretical studies either
38 addressed the CR or CP mechanisms individually, or considered both effects simultaneously in
39
40
41
42
43
44
45
46
47
48
49
50
51
52
53
54
55
56
57
58
59
60

1
2
3 simplified models that did not include the details of protein structures (*i.e.* the positions of the
4 aminoacids in the three-dimensional space). Moreover, none of these studies provided a clear strategy
5
6 to isolate the relative thermodynamic contributions of CR and CP to the total adsorption free energy.
7
8 This work introduces a new theoretical method to calculate the thermodynamic properties and the
9
10 state of charge of the acid-base groups in a protein in the absence or presence of a surface. We first
11
12 validate our theoretical method by comparing its predictions with experimental titration curves and
13
14 experimental apparent pK_as values for individual aminoacids. Then, we propose, for the first time, a
15
16 strategy designed to isolate and analyze the relative importance of the CR and CP mechanisms on the
17
18 total adsorption free energy. Our results show that both effects are relevant at low ionic strengths,
19
20 while the CP mechanism dominates at high salt concentration. Moreover, we show that the
21
22 contribution of the CR effect is rather insensitive to protein orientation, which suggests that constant-
23
24 charge simulations (which neglect CR) can be used to predict protein orientation on a surface without
25
26 incurring in large errors. Finally, our study reveals that the presence of the surface can induce large
27
28 pK_a shifts in individual aminoacids, even for physiological salt concentrations (up to one pK_a unit
29
30 for a 0.1 M electrolyte). These pK_a shifts may have important implications for protein function in
31
32 biology and technology, for example for the catalytic behavior of enzymes near membranes or on
33
34 solid substrates, respectively. We present and validate a simple model that provides an explicit
35
36 expression to estimate the magnitude of the surface-induced pK_a shifts of all acid-base sites in a
37
38 protein. The input of the model is the distance between each site and the charged surface, which can
39
40 be determined from the knowledge of the protein structure and its orientation on the surface.
41
42
43
44
45
46
47
48
49
50

51 **Theoretical Approach**

52
53
54
55
56
57
58
59
60

Formulation of the Theoretical Method. We briefly discuss here our theoretical approach to study the different mechanisms involved in the interaction of proteins with a charged surface. The reader is referred to the Supporting Information (SI) for a detailed description of our method. We model the structure of a single protein in three dimensions at a coarse-grain level of description and fixed atomic positions. Our theory explicitly considers (at a mean-field level) the configurational space of the mobile ions and the state of ionization of all acid-base groups in the system. The theory can be used to model proteins both in solution and on charged surfaces.

Our theoretical approach is based on writing down an approximate grand-canonical free-energy functional (*i.e.* a grand potential functional) for the system. Note that the grand-canonical free energy, Ω , is the relevant quantity in the present system because the free ions in solution have a fixed chemical potential (including protons, *i.e.* we work at fixed pH) rather than a fixed number. The grand-canonical free energy is:

$$\begin{aligned}
 \beta\Omega [\rho_i(\mathbf{r}), \psi(\mathbf{r}), f_j] = & \sum_{i=H^+, OH^-, C^+, A^-} \int \rho_i(\mathbf{r}) [\ln(\rho_i(\mathbf{r}) / \rho^0) - 1 + \beta\mu_i^0] d\mathbf{r} + \\
 & \sum_{j = \text{all sites}} [f_j \ln(f_j) + (1 - f_j) \ln(1 - f_j) + \\
 & f_j \beta\mu_{j, \text{charged}}^0 + (1 - f_j) \beta\mu_{j, \text{uncharged}}^0] - \sum_{j = \text{acid sites}} [(1 - f_j) \beta\mu_{H^+}] \\
 & - \sum_{j = \text{basic sites}} [(1 - f_j) \beta\mu_{OH^-}] - \sum_{i=H^+, OH^-, C^+, A^-} \int \beta\mu_i \rho_i(\mathbf{r}) d\mathbf{r} \\
 & + \int \left[\langle \rho_Q(\mathbf{r}) \rangle \beta\psi(\mathbf{r}) - \frac{1}{2} \beta\epsilon(\mathbf{r}) (\nabla \psi(\mathbf{r}))^2 \right] d\mathbf{r} + \int_{surf} \sigma \beta\psi(\mathbf{r}) d\mathbf{r}
 \end{aligned} \tag{1}$$

where $\beta = (k_B T)^{-1}$, k_B is Boltzmann's constant and T is the absolute temperature (298 K). The grand potential Ω is a functional of $\rho_i(\mathbf{r})$, which is the number density of species i at the position \mathbf{r} in the system ($i = H^+$, OH^- , C^+ and A^- for protons, hydroxyl ions, cations and anions, respectively); f_j which is the average ionization state of the acid-base group j (*i.e.* the probability of having the group j in its

1
2
3 charged state) and $\psi(\mathbf{r})$, which is the electrostatic potential at position \mathbf{r} . Eq (1) contains contributions
4
5 from the mixing entropy of the ions and their standard chemical potentials (first term); the free energy
6
7 of the acid-base chemical equilibria for all acid-base groups in the system (second term); the $-N_i\mu_i$
8
9 terms of the grand potential, where N_i and μ_i are the number and chemical potential of ions of type i
10
11 (third, fourth and fifth terms) and the electrostatic contribution to the free energy³⁹ (sixth and seventh
12
13 terms).
14
15

16
17 The equilibrium structure of the system results from finding the extrema of eq (1) with respect to
18
19 $\rho_i(\mathbf{r})$, f_j and $\psi(\mathbf{r})$, which leads, after some rearrangements, to expressions for these unknowns. The
20
21 extremum with respect to $\rho_i(\mathbf{r})$ yields,
22
23

$$24 \quad \rho_i(\mathbf{r}) = \rho_i^{bulk} \exp(-\beta q_i \psi(\mathbf{r})) \quad (2)$$

25
26 where ρ_i^{bulk} is the bulk number density of species i (*i.e.* the density far away from the protein and the
27
28 charged surface) and q_i is the charge of species i . The functional extremum of $\beta\Omega$ with respect to $\psi(\mathbf{r})$
29
30 results in the Poisson equation,
31
32

$$33 \quad \nabla(\epsilon(\mathbf{r})\nabla\psi(\mathbf{r})) = -\langle\rho_Q(\mathbf{r})\rangle \quad (3)$$

34
35 where $\epsilon(\mathbf{r})$ is the static dielectric constant of the medium at \mathbf{r} and $\langle\rho_Q(\mathbf{r})\rangle$ is the average charge density
36
37 at \mathbf{r} , which has contributions from the charges of the ions and the acid-base groups of the protein.
38
39

40
41 The boundary condition of eq (3) at the bulk solution (solution far from the protein and the surface)
42
43 is $\psi^{bulk} = 0$ and the boundary condition at the charged surface (located in the y - z plane at $x = 0$) is:
44
45

$$46 \quad \frac{\partial\psi}{\partial x} = -\frac{\sigma}{\epsilon(\mathbf{r})} \quad (4)$$

47
48 where σ is the charge density of the surface.
49
50
51
52
53
54
55
56
57
58
59
60

1
2
3 Finally, the functional extremum with respect to f_j results in expressions for the acid-base equilibrium.

4
5 For example, for acidic groups, we obtain:

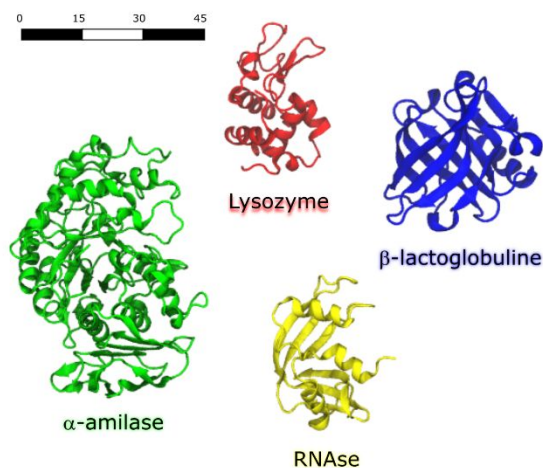
$$6 \quad \frac{f_j \rho_{H^+}^{bulk}}{1 - f_j} = \rho^\circ \exp(\beta |e| \bar{\psi}(\mathbf{r}_j^\circ)) \exp(-\beta \Delta\mu_j^\circ) \quad (5)$$

7
8
9
10
11
12 where ρ° is a reference density, $\bar{\psi}(\mathbf{r}_j^\circ)$ is the average of the electrostatic potential over the volume of
13
14
15 the acid group j (see SI), $|e|$ is the elemental charge and $\Delta\mu_j^\circ$ is the change in the standard free energy
16
17
18 associated with the charging reaction of the site j (acid deprotonation). The value of $\Delta\mu_j^\circ$ that should
19
20
21 be used in eq (5) depends on the choice of the reference state. A distinctive feature of our theory is
22
23
24 the method to obtain $\Delta\mu_j^\circ$ in order to guarantee the correct description of the reference state given by
25
26
27 a single acid-base group in the bulk. We first find the values of $\Delta\mu_j^\circ$ for all acid-base groups by
28
29
30 solving the theory for each of them isolated in the bulk and enforcing $f = 0.5$ when $\text{pH} = \text{pKa}$ (where
31
32
33 the pKa values used in these calculations are those experimentally determined and tabulated for the
34
35
36 side chains or terminal groups of the aminoacids, see SI). These calculations provide the values of
37
38
39 $\Delta\mu_j^\circ$ for all acid-base groups, which can then be used to solve the theory for the protein at any pH.

40
41
42 In order to solve the theory, equations (2)-(5) and the equation for the acid base equilibrium of basic
43
44
45 groups (see SI) are discretized in a grid and solved using numerical methods. This calculation
46
47
48 provides us with thermodynamic (Ω) and structural ($\psi(\mathbf{r}), \rho_i(\mathbf{r}), f_j$) information and allows us to
49
50
51 calculate the total charge of the protein as $Q_{tot} = \sum_{j=\text{all sites}} f_j q_j$, where q_j is the charge of the acid-base
52
53
54 group j in its charged state.

55
56
57 The inputs of the theory are the structure of the protein (which we obtained from the corresponding
58
59
60 pdb file from the Protein Data Bank); the properties of the solution (salt concentration and pH) and

1
2
3 the surface (surface charge density, σ); the pKas of the isolated aminoacids in the bulk and their
4 volumes (see Table S1 in the SI); the orientation of the protein on the surface, which is unequivocally
5 defined by two angles, φ and ϕ (the azimuthal and polar angles, respectively) and the dielectric
6 constants of the solvent and the protein. Additional details of the protein model and the discretization
7 and numerical solution of the theory are provided in the SI.
8
9
10
11
12
13
14
15
16
17



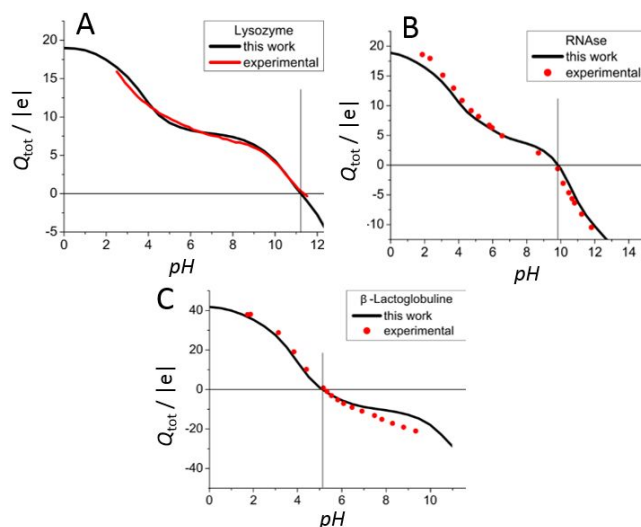
18
19
20
21
22
23
24
25
26
27
28
29
30
31
32
33
34 **Figure 1.** Representation of the proteins (as secondary structure) used in this work. The structures
35 were obtained from crystallographic atomic coordinates taken from the PDB files: Hen egg-white
36 lysozyme (in red, IEP: 11.2, PDB ID: 3RZ4), RNase (ribonuclease A, in yellow, IEP: 9.9, PDB Id:
37 lysozyme (in red, IEP: 11.2, PDB ID: 3RZ4), RNase (ribonuclease A, in yellow, IEP: 9.9, PDB Id:
38 1KF5 ⁴⁰), human salivary α -amylase (in green, IEP: 6.4, PDB Id: 1SMD ⁴¹) and ovine β -
39 lactoglobuline (in blue, IEP: 5.1, PDB: 4CK4 ⁴²). The bar shows the scale in Angstroms.
40
41
42
43
44
45

46 **Results and Discussion**

47
48 **Validation of the Theoretical Methodology.** Figure 1 shows the secondary structure of the proteins
49 selected for this study: lysozyme, α -amylase, RNase and β -lactoglobuline. These four proteins span
50 a wide range of molecular sizes, types of folding and isoelectric points (IEP). We chose lysozyme,
51 RNase and β -lactoglobuline due to the availability of experimental titration curves and/or single-
52
53
54
55
56
57
58
59
60

1
2
3 aminoacid pKa values. Since the most relevant conclusions of this work are of general validity, we
4 will mostly present results for lysozyme in the main text and refer the reader to the SI for selected
5
6 results of the other proteins.
7
8

9
10 In order to validate our theoretical approach, we calculated the titration curves (total protein charge,
11
12 Q_{tot} , vs pH) for lysozyme, β -lactoglobuline and RNase and compared them with the experimental
13
14 titration curves from literature, see Figure 2. We observe a good agreement between theory and
15
16 experiment for lysozyme and RNase in the whole pH range under study. In the case of β -
17
18 lactoglobuline, a good agreement is observed for acidic pHs, although our prediction deviates from
19
20 the experimental results for $\text{pH} > 5$. We speculate that this discrepancy may arise from the fact that
21
22 the crystallographic structure of β -lactoglobuline used in the calculations corresponds to a sample
23
24 crystallized at $\text{pH} 5.6$,⁴² but β -lactoglobuline is known to undergo conformational changes above pH
25
26 4.5, followed by unfolding above $\text{pH} 9$.^{43,44} Therefore, the structure used in our calculations may
27
28 appreciably differ from that present in solution for $\text{pH} > 5$.
29
30
31
32



51 **Figure 2.** Comparison of experimental and calculated titration curves (net protein charge, Q_{tot} , vs pH)
52 for lysozyme (A, experimental data was originally plotted as a solid line),⁴⁵ RNase (B)⁴⁶ and β -
53
54
55

1
2
3 lactoglobuline (C).⁴³ The isoelectric point (IEP) of each protein ($Q_{\text{tot}}=0$) is indicated with straight
4
5 lines.

6
7
8 As an additional validation, we applied our methodology to calculate the apparent pKas, pKas^{app} , of
9
10 each titratable aminoacid in lysozyme (the pKas^{app} of an acid-base site is defined as the solution pH
11
12 for which the site has an average ionization fraction of $f = 0.5$.) Lysozyme is usually used to
13
14 benchmark the performance of pKa calculations^{28,35,36} because the pKas^{app} of most of its aminoacids
15
16 have been experimentally determined⁴⁷ and because this enzyme is very stable to changes of
17
18 temperature, pH and salt concentration. Our results (see Figure S2 in the SI) show an average
19
20 difference of 0.87 pKa units between the pKas^{app} predicted by our method and the experimental
21
22 values. This difference is similar to those obtained with other pKa calculation programs: PropKa³⁷
23
24 (0.95), Fambe-pH³⁵ (1.16) and Delphi³⁴ (0.75).

25
26
27 So far, we showed that our method can correctly predict titration curves in bulk and the apparent
28
29 pKas of individual aminoacids with the same level of accuracy as other methods in literature. A key
30
31 advantage of our method, compared with available pKa-predicting tools, is that it allows to
32
33 straightforwardly incorporate the presence of a charged surface in the system.

34
35
36 **Interaction between Isoelectric Proteins and Charged Surfaces.** Let us consider the interaction
37
38 between proteins that are at their isoelectric point (IEP) and thus have zero net charge in bulk
39
40 (isoelectric proteins) with charged surfaces. We first determine the grand-canonical free energy of
41
42 adsorption $\Delta\Omega^{\text{ads}}$, defined as

$$43 \Delta\Omega^{\text{ads}} = \Omega^{\text{prot/surf}} - \Omega^{\text{prot/sol}} - \Omega^{\text{surf}} \quad (6)$$

44
45 where $\Omega^{\text{prot/surf}}$, $\Omega^{\text{prot/sol}}$ and Ω^{surf} are the free energies (determined with eq (1)) of the protein-surface
46
47 system, the protein in the bulk solution and the surface in the absence of the protein, respectively. It
48
49 is worthwhile to recall, that in this work we are interested in studying the electrostatic contribution to
50
51
52
53
54
55
56
57
58
59
60

1
2
3 the adsorption free energy (where ‘electrostatic contribution’ is broadly defined and includes effects
4 such as counter-ion release and charge regulation). Therefore, the functional Ω (eq (1)), and the values
5
6 of $\Delta\Omega^{ads}$ derived from it, contain only contributions from the electrostatic energy, mixing entropies of
7
8 the free ions and the free-energy contributions from chemical equilibria. They do not include other
9
10 contributions, such as protein-surface hydrogen bonds and hydrophobic interactions, which also
11
12 contribute to the thermodynamics of the adsorption⁶ (unlike the electrostatic interactions, these
13
14 contributions are very dependent on the chemical nature of the surface⁴⁸). Therefore, $\Delta\Omega^{ads}$ does not
15
16 allow to unequivocally predict whether adsorption will occur or not, but it rather indicates whether
17
18 electrostatic interactions favor adsorption or not.
19

20
21 Since $\Delta\Omega^{ads}$ depends on the orientation of the protein and its distance from the surface, we performed
22
23 calculations fixing the distance between the surface and the center of the bead closest to it to 0.6 nm
24
25 and we sampled the orientational space of the protein on the surface by considering 404 different
26
27 orientations, each one characterized by two rotation angles, φ and ϕ , see SI. Figure 3 shows color
28
29 maps of $\Delta\Omega^{ads}$ as a function of φ and ϕ for the adsorption of lysozyme at different ionic strengths
30
31 and on negative and positive surfaces (similar plots for the other proteins are presented in Figures S3,
32
33 S4 and S5 in the SI). In all calculations, we used a surface charge density, $\sigma = -1 \text{ |e|}\cdot\text{nm}^{-2}$ (negative
34
35 surfaces) or $1 \text{ |e|}\cdot\text{nm}^{-2}$ (positive surfaces) that is in the same order of magnitude as model silica
36
37 surfaces, which have $\sigma = -2.6 \text{ |e|}\cdot\text{nm}^{-2}$.³¹ We observe that $\Delta\Omega^{ads}$ strongly depends on protein
38
39 orientation. For some orientations, $\Delta\Omega^{ads}$ is negative, indicating a favorable electrostatic contribution
40
41 to the adsorption of the isoelectric protein. As expected for an attraction of electrostatic nature, the
42
43 minima of $\Delta\Omega^{ads}$ become less negative as the added salt concentration increases (see scales of the
44
45 color maps in Figure 3). The effect of the sign of the surface charge and concentration of added salt
46
47
48
49
50
51
52
53
54
55
56
57
58
59
60

on protein adsorption shows some interesting features: i) the maxima in the plots for the positive surface are close to, but not exactly in the same position as, the minima in the plots of the negative surface (and *viceversa*) ii) the most stable orientation on a given surface changes with the concentration of added salt. These two effects are a consequence from the complex interplay between electrostatic attractions and repulsions in the system, which is modulated by charge regulation and the screening of charges by the electrolyte.

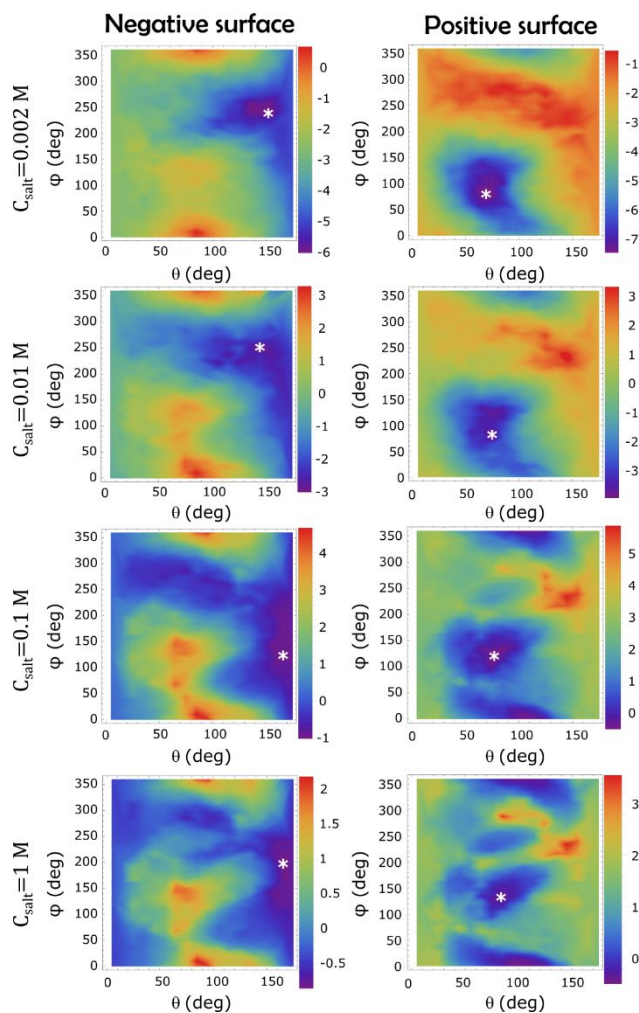


Figure 3. Color maps showing the adsorption (grand canonical) free energy, $\Delta\Omega^{ads}$ for lysozyme (in units of $k_B T$) as a function of the angles φ (azimuthal angle, y-axis) and θ (polar angle, x-axis), which determine the orientation of the protein on the surface. The plots correspond to negatively (left panels,

1
2
3 $\sigma = -1 \text{ |e|}\cdot\text{nm}^{-2}$) and positively (right panels, $\sigma = 1 \text{ |e|}\cdot\text{nm}^{-2}$) charged surfaces and different
4 concentrations of added 1:1 electrolyte, C_{salt} . White asterisks indicate the orientations of the protein
5
6 with the lowest $\Delta\Omega^{\text{ads}}$ for each plot.
7
8
9

11 **Analysis of Lysozyme-Surface Interaction**

12
13 We will now provide a detailed analysis of the determinants of protein adsorption for a selected case.
14
15 Figure 4A and 4B show color maps of the average charge density of lysozyme in solution (in units of
16 elemental charges per nm^3) for $\text{pH} = \text{IEP}$ and $C_{\text{salt}} = 2 \text{ mM}$. Let us now consider the interaction of
17
18 lysozyme with a negatively charged surface. The bottom view (Figure 4B) shows the side of lysozyme
19
20 that will face the surface for the orientation with minimal $\Delta\Omega^{\text{ads}}$ (orientation indicated with an
21
22 asterisk in the topmost right panel of Figure 3). Figures 4E and 4F indicate with red dots the positions
23
24 of the aminoacids that are relevant for the lysozyme-surface interaction. Note that each of these
25
26 aminoacids corresponds to a positive charge density (red spot) in Figures 4A and 4B. The aminoacids
27
28 Arg114, Arg125, Arg128, Arg5 and Lys1 are very close to the surface and almost fully dissociated;
29
30 therefore, these aminoacids contribute the most to the protein-surface attraction. Other aminoacids
31
32 that are almost fully dissociated are Arg45 and Arg112, but they are farther from the surface than the
33
34 other five aminoacids mentioned above.
35
36
37
38
39
40
41
42
43
44
45
46
47
48
49
50
51
52
53
54
55
56
57
58
59
60

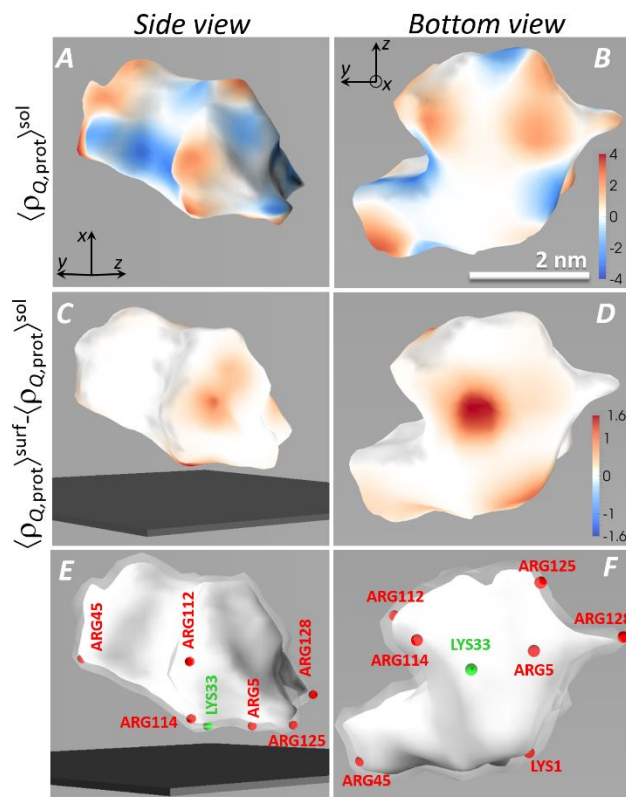


Figure 4. A, B. Color map of the charge density of the aminoacids of lysozyme in the bulk, $\langle \rho_{Q, \text{prot}} \rangle^{\text{sol}}$ (units of $|e| \cdot \text{nm}^{-3}$). Red and blue regions indicate positive and negative charge densities, respectively. The bottom view (panel B) shows the side of lysozyme that will interact with the charged surface. C, D. Color maps showing the change of the charge density of the aminoacids of lysozyme upon introducing the negatively charged surface, $\langle \rho_{Q, \text{prot}} \rangle^{\text{surf}} - \langle \rho_{Q, \text{prot}} \rangle^{\text{sol}}$. Red regions indicate an increase of the charge density upon adsorption. E, F. Plots showing the position of some relevant aminoacids on the surface of lysozyme.

Upon protein adsorption on the negatively charged surface, the aminoacids regulate their charge in response to the charge of the surface. The negatively charged surface inhibits the dissociation of negatively charged aminoacids and enhances the ionization of positive ones. This charge regulation (CR) mechanism results in an increase of the net charge of the protein, which favors protein adsorption. It is important to stress that the CR mechanism cannot be understood in terms of the

1
2
3 charge density of the aminoacids within the protein in bulk solution, but rather it is necessary to
4
5 examine the charge of lysozyme in the presence of the surface. Figures 4C and 4D, depict color maps
6
7 of the change in the charge density of the protein induced by the presence of the negative surface (red
8
9 spots indicate an increase of the charge density upon adsorption). Notably, Lys33 (indicated with a
10
11 green spot in Figures 4E and 4F) resides very close to the surface and its degree of ionization for pH
12
13 = IEP changes from weakly dissociated ($f = 0.09$) in solution, to strongly dissociated ($f = 0.72$) in the
14
15 presence of the surface. Therefore, it is very interesting that Lys33 strongly contributes to the
16
17 adsorption process, even though it is only weakly charged in the bulk protein.
18
19

20
21 It is worthwhile to compare the results in Figure 4 with the predictions of constant-charge MD
22
23 simulations in literature, which modelled the adsorption of lysozyme on negatively charged silica
24
25 surfaces at pH 7^{49,50} and 8.⁵¹ The orientation predicted by our model for lysozyme at its isoelectric
26
27 point (pH 11.2) on a negative surface is very close to the most stable orientation predicted by these
28
29 MD simulations.^{49–52} Moreover, MD studies have identified the same aminoacids as our study (Lys1,
30
31 Arg5, Arg125 and Arg128) as the aminoacids that reside closest to the surface and contribute the
32
33 most to the interaction with the silica substrate.
34
35

36
37 In Figure 5, we analyze the CR effect in further detail. Figures 5A and 5B show the titration curves
38
39 (total protein charge, Q_{tot} , vs pH) for lysozyme in solution and in the presence of the negatively
40
41 charged surface for total ionic strengths of $I = 2$ mM (Fig 5A) and 100 mM (Fig. 5B). For $I = 2$ mM,
42
43 lysozyme on the surface has between one to four positive charges (depending on the pH) more than
44
45 lysozyme in solution, which shows a strong CR effect. On the other hand, for $I = 100$ mM the
46
47 differences between the bulk and the surface titration curves are very slight, but the CR effect is still
48
49 operative and it still can produce important shifts in the apparent pKas of individual aminoacids. This
50
51 effect is demonstrated in Figure 5C, which shows the degree of ionization, f , as a function of pH for
52
53
54
55
56
57
58
59
60

1
2
3 Lys33 and Asp119 in lysozyme in solution and on a negative surface for $I = 100$ mM. Interestingly,
4 even at this relatively large ionic strength, there are large shifts in the pKas^{app} of the aminoacids upon
5 adsorption: $\Delta\text{pKa}^{\text{app}} = +0.89$ for Lys33 and $+0.60$ for Asp119, where we defined $\Delta\text{pKa}^{\text{app}} = \text{pKa}^{\text{app,surf}}$
6 $- \text{pKa}^{\text{app,sol}}$, see Figure 5C. Surface-induced pKa shifts can be very important for enzymes whose
7 catalytic activity relies on the acid-base properties of the aminoacids in the active site.^{53–55} In this
8 type of enzymes, one can expect that shifts in the apparent pKas of the aminoacids in the active site
9 upon adsorption will affect the catalytic efficiency and/or shift the pH of optimal catalytic activity of
10 the enzyme.^{3,56,57}

11
12 So far, we have shown that the charge of the surface induces shifts in the pKa^{app} of the aminoacids
13 upon adsorption (up to one pKa unit). The magnitude of these shifts (*i.e.* the magnitude of $\Delta\text{pKa}^{\text{app}}$)
14 is expected to decrease for increasing distance between the aminoacid and the surface. This prediction
15 is confirmed in Figure 5D which shows $\Delta\text{pKa}^{\text{app}}$ for different aminoacids as a function of the distance
16 of the aminoacid from the surface for $I = 100$ mM (some arginines that have $\text{pKas}^{\text{app}} > 13$ are not
17 included in the plot).

18
19 The trend observed in Figure 5D can be captured by a simple model that considers the effect of the
20 local electrostatic potential on the pKa^{app} . The model, which is derived in the SI, relates the surface-
21 induced pKa^{app} shift of an aminoacid with its distance to the charged surface, x :

$$22 \Delta\text{pKa}^{\text{app}} =$$

$$23 1.74 \cdot \text{atanh} \left[\tanh \left(\frac{1}{2} \text{asinh} \left(\frac{\sigma}{(8l\epsilon k_B T)^{1/2}} \right) \right) \exp(-\kappa x) \right] \quad (7)$$

24 where κ is the Debye length of the solution and ϵ is the dielectric constant of the medium.

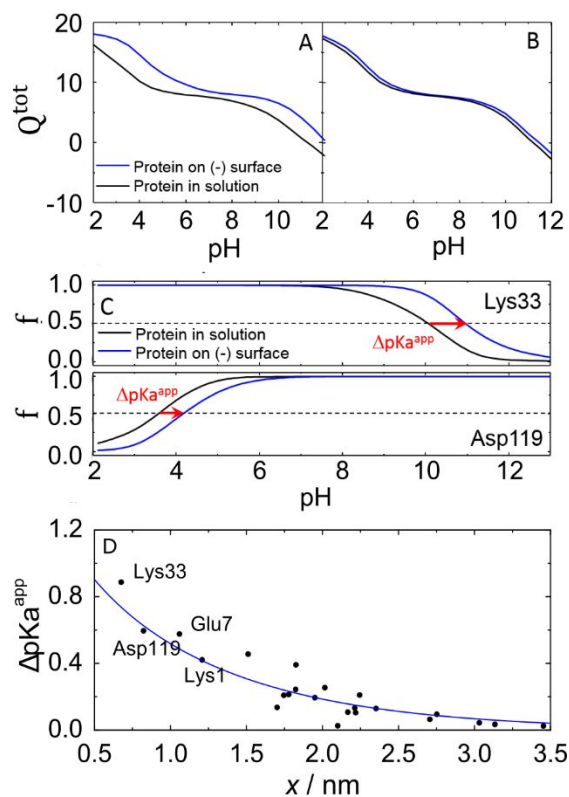


Figure 5. A, B. Titration curves (total protein charge vs pH) for lysozyme in bulk (black line) and on a negatively charged surface (blue line) for ionic strengths of 2 mM (A) and 100 mM (B). C. Titration curves (average fraction of ionization, f , vs pH) for Lys33 and Asp119 for an ionic strength of 100 mM. The plots show titration curves for the aminoacids inside lysozyme in bulk solution (black line) and on a negatively charged surface (blue line). The changes of the apparent pKas upon adsorption, ΔpK_a^{app} , are shown with horizontal red arrows. D. Change in pK_a^{app} upon adsorption, ΔpK_a^{app} , as a function of the distance from the charged surface, x , for the aminoacids in lysozyme. The blue solid line shows the prediction of eq (7). In all cases, the orientation of lysozyme on the surface corresponds to that with the minimal adsorption free energy (minimal $\Delta\Omega^{\text{ads}}$ in the corresponding plots of Figure 3)

The prediction of eq (7) is shown with a blue solid line in Figure 5D. The simple model captures very well the general trend displayed by the more detailed calculations of our theoretical method. The

differences between the predictions of eq (7) and those of our theoretical method are due to the local environment of each aminoacid inside the protein. We believe that eq (7) can be used by experimental groups working with adsorbed proteins to estimate the magnitude of surface-induced pK_a^{app} shifts of single aminoacids. The main difficulty in using the equation is to determine the distance between the aminoacid and the surface. We suggest that this parameter can be estimated by combining the crystallographic structure of the protein (*i.e.* obtained from PDB files) with experimental or theoretical information about its orientation on the substrate.

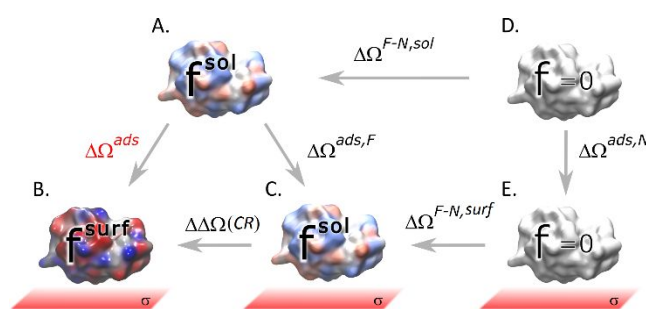


Figure 6. Thermodynamic cycle used to study the contributions from CR and CP to the adsorption of isoelectric proteins onto charged surfaces. The states represented in the cycle correspond to: A. protein far from the charged surface (*i.e.* in the bulk solution); B. protein on a charged surface, where the average state of ionization of each aminoacid changes with respect to state A due to the charge-regulation mechanism; C. hypothetical state where the protein is placed on the charged surface, but it retains the same state of charge as the protein in the solution (*i.e.* same charge state as the protein in state A); D. Protein in solution in a hypothetical state where all acid-base groups are non-ionized; E. Same as D, but for the protein on a charged surface.

Analysis of the Contributions from Charge Regulation (CR) and Charge Patches (CP) to Protein Adsorption. We will address in this section the different contributions to $\Delta\Omega^{ads}$, with special

1
2
3 focus on the relative strength of two electrostatic mechanisms that promote the adsorption of proteins:
4 charge regulation (CR) and charge patches (CP). It is worthwhile to mention that these contributions
5 are not explicit terms in our free energy functional, eq (1), and they can only be extracted from our
6 theory by comparing the free energies of different states of the protein/surface system. For this
7 purpose, we devised the thermodynamic cycle in Figure 6. This cycle relates different states of the
8 system. Some of them are hypothetical states that do not correspond to real states of the
9 protein/surface system. The charge distribution of the protein in each state in Figure 6 is
10 unequivocally defined by the values of the average fractions of ionization of all acid-base groups, *i.e.*
11 the values of f_j for all j . We will refer to this set of values as \mathbf{f} . The free-energy differences between
12 the different states in Figure 6 are calculated using our theoretical method, as described in the
13 Methods Section, although in the hypothetical states \mathbf{f} is fixed to a given value instead of determined
14 from the theory (*i.e.* by solving eq (5) for acidic groups or the equivalent equation for basic groups).
15 In other words, in these hypothetical states the free energy is no longer required to be an extrema with
16 respect to the ionization fractions f_j .

17
18
19
20
21
22
23
24
25
26
27
28
29
30
31
32
33
34
35
36
37
38
39
40
41
42
43
44
45
46
47
48
49
50
51
52
53
54
55
56
57
58
59
60

The state A in Figure 6 corresponds to the protein very far from the charged surface (charge state \mathbf{f}^{sol}) and the state B corresponds to the protein on the charged surface (charge state \mathbf{f}^{surf}). The change of the grand-canonical free energy Ω between states A and B is $\Delta\Omega^{\text{ads}}$, which has been already defined in eq (6) and discussed in Figure 3. State C in Figure 6 is an hypothetical state in which the protein is located on the surface but it keeps the same state of charge as in bulk solution (*i.e.* it has a charge state \mathbf{f}^{sol}). The free-energy difference between states C and A is, therefore, the free energy of adsorption of a protein that cannot regulate its charge, which we denote $\Delta\Omega^{\text{ads},F}$ (where the superscript F indicates fixed charge). Based on these definitions, we identify the contribution of charge regulation to the total adsorption free energy as:

$$\Delta\Delta\Omega(CR) = \Delta\Omega^{ads} - \Delta\Omega^{ads,F} \quad (8)$$

States D and E in the cycle of Figure 6 are hypothetical states of a protein far from the surface (state D) or on the surface (state E) in which the charges of all aminoacids have been set to zero (*i.e.* $\mathbf{f} = 0$). Note that this situation differs from that in states A and B, where the net protein charge is zero (because $\text{pH} = \text{IEP}$), but each acid-base group has a non-zero average charge. The free-energy difference between states D and E is $\Delta\Omega^{ads,N}$, which is an adsorption free energy for a hypothetical protein that have non-ionized acid-base groups. The value of $\Delta\Omega^{ads,N}$ is always positive (*i.e.* favors protein-surface repulsion) because of the combination of two effects: i) placing a protein with $\mathbf{f} = 0$ near the charged surface displaces the counterions that are compensating the charge of the surface, which results in an increase in system's free energy, ii) the protein has a dielectric constant smaller than the solvent, thus placing it in the electric field generated by the surface results in an energetic penalty. Additional calculations (presented in Figure S6 in the Supporting Information) show that the first mechanism (disruption of electrical double layer by the protein) accounts for 72%-85% of the total value of $\Delta\Omega^{ads,N}$.

At this point, we can isolate the contribution of charge patches to the total adsorption free energy, $\Delta\Delta\Omega(CP)$. This contribution is equal to the adsorption free energy of the hypothetical protein with non-regulating acid-base groups (*i.e.* a protein that has charge patches but cannot regulate charge), $\Delta\Omega^{ads,F}$, minus the adsorption free energy of the protein with fully non-ionized acid-base groups, $\Delta\Omega^{ads,N}$:

$$\Delta\Delta\Omega(CP) = \Delta\Omega^{ads,F} - \Delta\Omega^{ads,N} \quad (9)$$

Analysis of the thermodynamic cycle in Figure 6 provides an alternative definition of $\Delta\Delta\Omega(CP)$:

$$\Delta\Delta\Omega(CP) = \Delta\Omega^{F-N,surf} - \Delta\Omega^{F-N,sol} \quad (10)$$

1
2
3 where $\Delta\Omega^{F-N,surf}$ and $\Delta\Omega^{F-N,sol}$ are the free-energy changes due to introducing the charge patches
4
5 (changing the state of charge from $\mathbf{f} = 0$ to \mathbf{f}^{sol}) in a protein on the surface and in a protein in solution,
6
7 respectively. Therefore, according to this definition, $\Delta\Delta\Omega(CP)$ is the difference between the free
8
9 energy of introducing the charge patches in a protein on the surface and the free energy of introducing
10
11 them in a protein in the solution.
12
13

14
15 Adding eqs (8) and (9) results in:

$$\Delta\Omega^{ads} = \Delta\Delta\Omega(CR) + \Delta\Delta\Omega(CP) + \Delta\Omega^{ads,N} \quad (11)$$

16
17
18
19
20 which shows that the total adsorption free energy can be split into three contributions: one from
21
22 charge regulation, $\Delta\Delta\Omega(CR)$; one from charge patches, $\Delta\Delta\Omega(CP)$ and one from the adsorption of a
23
24 neutral protein, $\Delta\Omega^{ads,N}$. Equation (11) is the most important result from the thermodynamic cycle in
25
26 Figure 6 because it shows that the total adsorption free energy in our theory can be split into three
27
28 contributions that are attributable to well-defined processes.
29
30

31
32 In Figure 7, we plot $\Delta\Delta\Omega(CR)$, $\Delta\Delta\Omega(CP)$ and $\Delta\Omega^{ads,N}$ as a function of $\Delta\Omega^{ads}$ for lysozyme under the
33
34 same conditions of Figure 3 (positive and negative surfaces and four different concentrations of added
35
36 salt). Note that each point in the plots of Figure 7 corresponds to a different orientation of the protein
37
38 on the surface. The most stable orientations (points with minimal $\Delta\Omega^{ads}$) are, therefore, located on
39
40 the left side of each plot.
41
42

43
44 As we explained above, the contribution from the adsorption of the neutral protein, $\Delta\Omega^{ads,N}$, is always
45
46 positive. It is also rather insensitive to protein orientation because it depends only on the volume
47
48 distribution of the protein along the direction normal to the surface. This volume distribution does
49
50 not change too much with protein orientation unless the protein is highly elongated.
51
52
53
54
55
56
57
58
59
60

1
2
3 The contribution from charge regulation, $\Delta\Delta\Omega(CR)$, is always negative and similar for all orientations.
4
5 We attribute the insensitiveness of $\Delta\Delta\Omega(CR)$ with orientation to the fact that all aminoacids in the
6
7 protein can regulate charge (although differently, depending on their pK_a^{app} and solution pH).
8
9 Therefore, in all orientations there are aminoacids close to the surface that can contribute to $\Delta\Delta\Omega(CR)$.
10
11 At this point, it is useful to highlight that most MD simulations aiming to determine the orientation
12
13 of proteins on surfaces use fixed charges and, therefore, neglect CR effects. The fact that $\Delta\Delta\Omega(CR)$ is
14
15 relatively insensitive to protein orientation suggests that fixed-charge MD do not introduce an
16
17 important error by neglecting CR when comparing the relative stability of different protein
18
19 orientations, thus validating the use of constant-charge simulations for this purpose. Furthermore, the
20
21 insensitiveness of $\Delta\Delta\Omega(CR)$ with protein orientation observed in Figure 7 for $pH = IEP$ is maintained
22
23 even when the protein has a non-zero charge in solution (pH not equal to IEP), see below.
24
25
26
27
28
29
30
31
32
33
34
35
36
37
38
39
40
41
42
43
44
45
46
47
48
49
50
51
52
53
54
55
56
57
58
59
60

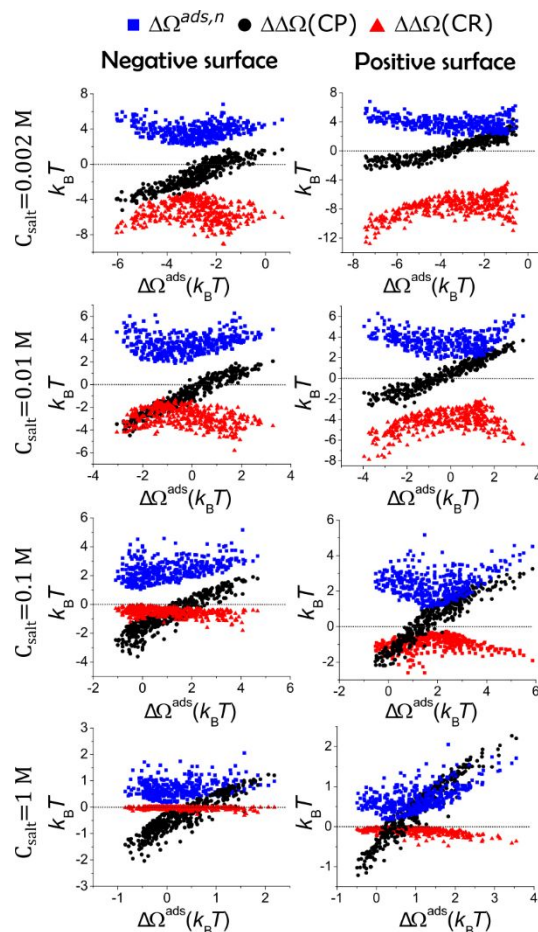


Figure 7. Contribution from charge patches ($\Delta\Delta\Omega(CP)$, black circles), charge regulation ($\Delta\Delta\Omega(CR)$, red triangles) and free-energy of adsorption of neutral protein ($\Delta\Omega^{ads,N}$, blue squares) to the adsorption free energy as a function of the total adsorption free energy, $\Delta\Omega^{ads}$. Each point corresponds to a different orientation of the protein on the surface. The plots correspond to lysozyme at pH = IEP for the same conditions as in Figure 3.

The contribution from CP, $\Delta\Delta\Omega(CP)$, strongly depends on protein orientation and it can be either positive or negative. There is a strong linear correlation between $\Delta\Delta\Omega(CP)$ and $\Delta\Omega^{ads}$, which indicates that $\Delta\Delta\Omega(CP)$ is the main responsible for determining the most favorable orientation on the surface.

1
2
3 At this point we ask the question of which mechanism, CP or CR, contributes the most to the
4
5 adsorption free energy of isoelectric proteins. The contributions to $\Delta\Omega^{ads}$ for the most stable
6
7 orientation (orientations with most negative $\Delta\Omega^{ads}$) in each panel of Figure 7 show that the answer to
8
9 this question depends on the salt concentration of the solution. For low salt concentration (2 mM),
10
11 both CP and CR contribute to protein adsorption, with charge regulation accounting for $\sim 80\%$ of the
12
13 total stabilization free-energy ($\Delta\Delta\Omega(CP) + \Delta\Delta\Omega(CR)$) for the negative surface and $\sim 65\%$ for the
14
15 positive surface. On the other hand, for high concentration of added salt (1.0 M), the CR contribution
16
17 is almost zero and, therefore, the CP contribution dominates. The CR effect vanishes at high ionic
18
19 strength because its magnitude depends on the intensity of the electrostatic potential generated by the
20
21 surface at the position of the acid-base group, see eq (7). Therefore, as the ionic strength of the
22
23 solution increases, salt ions screen the charge of the surface and decrease the magnitude of the local
24
25 electrostatic potential at the position of the acid-base groups. As a consequence, the charge regulation
26
27 effect weakens and $\Delta\Delta\Omega(CR)$ approaches zero. Note that the contribution due to charge patches,
28
29 $\Delta\Delta\Omega(CP)$, also decreases in magnitude upon increasing the ionic strength of the solution, but this
30
31 decrease is less dramatic than that of $\Delta\Delta\Omega(CR)$. In other words, while both mechanisms, CR and CP,
32
33 depend on the magnitude of the electrostatic potential at the position of the protein, the CR effect is
34
35 more affected by this variable than the CP mechanism.
36
37
38
39
40
41
42
43

44 The conclusions reached so far for lysozyme are valid for the other proteins as well. Figure 8
45
46 compares the different contributions to $\Delta\Omega^{ads}$ for the four proteins considered in this study on
47
48 negatively charged surfaces for salt concentrations of 2 mM and 1.0 M. We observe that the results
49
50 for all proteins qualitatively follow the same trends discussed in Figure 7 for lysozyme. Figures S7,
51
52
53
54
55
56
57
58
59
60

1
2
3 S8 and S9 in the Supporting Information show additional plots for β -lactoglobuline, α -amilase and
4
5 RNAsa for other salt concentrations and positively charged surfaces.
6

7
8 We finally briefly address the case discussed in the introduction where the protein has a net charge
9
10 of the same sign as that of the surface, *i.e.* the problem of protein adsorption in the ‘wrong side’ of
11
12 the isoelectric point. In Figure 9, we analyzed the adsorption of β -lactoglobuline on negatively
13
14 charged surfaces at pH 5.8, where the net charge in solution is $-2 |e|$ (the IEP of β -lactoglobuline is
15
16 5.1). Most of the conclusions obtained in Figure 7 for the isoelectric protein hold for the case of a
17
18 protein with the same charge as the surface: i) there are orientations on the surface that have $\Delta\Omega^{ads} <$
19
20 0 , thus electrostatics favor adsorption even in the ‘wrong side’ of the IEP; ii) the contribution of the
21
22 CR effect is rather insensitive to protein orientation and strongly decreases with increasing salt
23
24 concentration, iii) the CP effect is still responsible of dictating the most stable orientation for the
25
26 protein on the surface. Note that at low ionic strength, the magnitude of the CR effect is similar to
27
28 that observed for the isoelectric protein for β -lactoglobuline in Figure 9.
29
30
31
32
33
34
35
36
37
38
39
40
41
42
43
44
45
46
47
48
49
50
51
52
53
54
55
56
57
58
59
60

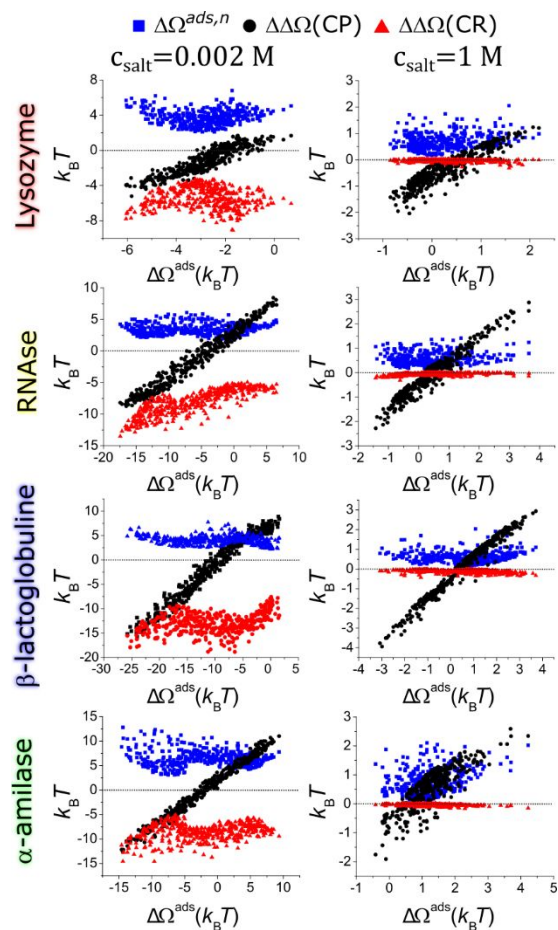


Figure 8. Same as Figure 7 for different proteins adsorbed on negatively charged surfaces ($\sigma = -1 \text{ |e|}\cdot\text{nm}^{-2}$) and salt concentrations of 2 mM (left panels) and 1 M (right panels).

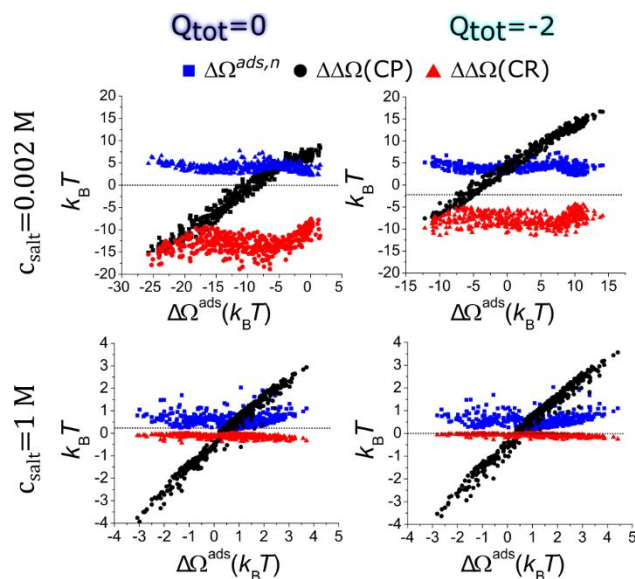


Figure 9. Comparison of the CP and CR contributions to the adsorption of β -lactoglobuline on negatively charged surfaces ($\sigma = -1 \text{ |e|}\cdot\text{nm}^{-2}$) for $Q_{\text{tot}}=-2 \text{ |e|}$ (pH 5.8) and $Q_{\text{tot}}=0$ (pH 5.1) for salt concentrations of 2 mM and 1 M.

It is worthwhile to mention that in the analysis of Figure 9, we kept the same definitions for the components of $\Delta\Omega^{\text{ads}}$ used for isoelectric proteins; therefore $\Delta\Delta\Omega(\text{CP})$ now accounts for the free energy of both bringing the net charge of the protein from 0 to -2 |e| and introducing the charge patches (the separation of these two processes is possible although not free of ambiguities and it will not be discussed in this work). However, it is worthwhile to note that the difference of $\Delta\Delta\Omega(\text{CP})$ between the most stable and the least stable orientations for β -lactoglobuline is similar for a net charge of -2 |e| (Figure 9, lower and upper right panels) and a net charge of zero (Figure 9, lower and upper left panels). This result suggests that the stabilization due to charge patches is similar in both cases; therefore, our conclusion that the CP contribution is similar to CR at low ionic strength and dominates at high ionic strengths also holds for proteins in the ‘wrong side’ of the isoelectric point.

Conclusions

In this work, we introduced a new theoretical framework to study the acid-base and electrostatic properties of proteins and validated it against experimental titration curves and pK_{as}^{app} values. While there exists several methods in literature for predicting the pK_{as}^{app} of aminoacids within proteins, our method has the key advantage of allowing to easily incorporate the presence of a surface in the calculations. Our method is also computationally efficient, for instance in this work we performed systematic calculations for four different proteins, 404 orientations, two types of surfaces (positive and negative), four different concentrations of added salt and seven different states (the states in the thermodynamic cycle of Figure 6), which accounts for a total of $\sim 9 \cdot 10^4$ different cases. Systematic studies of this size would be prohibitive with more accurate (and more expensive) calculation methods, such as constant-pH MD simulations.

We combined our theoretical framework with a strategy designed to isolate the contributions from the CR and CP mechanisms to the total adsorption free energy. This theoretical development allowed us to address for the first time the competition between CR and CP in a realistic protein model. Interestingly, the predictions of our study show some differences from those in previous works, which analyzed protein adsorption on soft surfaces using other levels of theoretical approximation.^{19,38} For example, these works suggested that the CR mechanism was the largest contribution to the free energy of adsorption at low ionic strengths,^{19,38} while we show that for the adsorption on a planar charged surface, both the CR and CP mechanisms have similar relevance (for $C_{salt} = 2$ mM). In agreement with all previous literature reports, we found that the importance of the CR effect decreases for increasing ionic strength. Notably, we found that the magnitude of the CP effect also decreases with increasing salt concentration, although to lesser degree than the CR mechanism.

1
2
3 An interesting prediction of our study is that the contribution from the CR mechanism is rather
4 insensitive to the orientation of the protein on the surface, therefore the orientation is mainly
5 determined by the CP mechanism. This conclusion suggests that neglecting the CR effect when
6 predicting protein orientations on a surface (which is the rule in constant-charge MD simulations) is
7 a good approximation. Note, however, that neglecting CR can still result in an incorrect picture of the
8 adsorption mechanism, for example in Figure 4, we show that Lys33 contributes to the adsorption of
9 Lysozyme onto a negatively charged surface, even when this aminoacid is uncharged in bulk solution.
10 This information is inaccessible to constant-charge calculations.

11
12 We showed that the effect of the surface on the pK_a^{app} of individual aminoacids decays with
13 increasing distance to the surface and we provided an explicit expression (eq (7)) that captures the
14 effect. Surface-induced pK_a^{app} shifts for functional aminoacids, such as those involved in enzymatic
15 catalytic sites, can be very important for the behavior of immobilized proteins. Our expression will
16 allow to estimate the magnitude of the effect, provided that the position of each aminoacid can be
17 estimated from the structure of the protein (*e.g.* from the protein data bank) and knowledge of the
18 orientation of the protein on the surface.

19
20 In future work, we plan to extend the capabilities of our theoretical framework to study some poorly
21 understood phenomena, such as protein adsorption on porous and nanomaterials, the effect of inter-
22 protein interactions on adsorption (which is a relevant problem under high-surface-coverage
23 conditions) and the effect of adsorption on the functional properties of the proteins.

24 ASSOCIATED CONTENT

25
26 **Supporting Information.** Detailed description of theoretical methods, comparison between all-atom
27 and coarse-grained representations of lysozyme, comparison between theoretical predictions and
28 experiments for the pK_a^{app} of aminoacids in lysozyme, adsorption free energy and its components for
29

1
2
3 β -lactoglobuline, RNase and α -amylase, derivation of eq 7, contributions to the free energy of
4 adsorption of neutral proteins and method to sample protein orientations on the surface. This material
5
6 is available free of charge via the Internet at <http://pubs.acs.org>.
7
8
9

10 AUTHOR INFORMATION

11 **Corresponding Author**

12
13
14
15
16 * Mario Tagliazucchi, email: mario@qi.fcen.uba.ar
17
18

19 **Author Contributions**

20
21
22 The manuscript was written through contributions of all authors. All authors have given approval to
23
24 the final version of the manuscript.
25
26
27

28 **Funding Sources**

29
30 Agencia Nacional de Promoción Científica y Tecnológica (AN-PCyT, PICT-2015-0099, PICT-
31
32 2016-0154, PICT-2015-3526, PAE-37063 PME-2006-00038)
33
34
35

36 University of Buenos Aires (UBACYT 20020170200215BA)
37
38

39 ACKNOWLEDGMENT

40
41 MT and GJAASI are fellows of CONICET. MT and GKAASI acknowledge support from Agencia
42
43 Nacional de Promoción Científica y Tecnológica (ANPCyT, PICT-2015-0099, PICT-2016-0154,
44
45 PICT-2015-3526, PAE-37063 PME-2006-00038) and Uni-versity of Buenos Aires (UBACYT
46
47 20020170200215BA).
48
49
50
51
52
53
54
55
56
57
58
59
60

REFERENCES

- (1) Hartmann, M. Ordered Mesoporous Materials for Bioadsorption and Biocatalysis. *Chem. Mater.* **2005**, *17* (18), 4577–4593.
- (2) Bhakta, S. A.; Evans, E.; Benavidez, T. E.; Garcia, C. D. Protein Adsorption onto Nanomaterials for the Development of Biosensors and Analytical Devices: A Review. *Anal. Chim. Acta* **2015**, *872*, 7–25.
- (3) Bellino, M. G.; Regazzoni, A. E.; Soler-Illia, G. J. A. A. Amylase-Functionalized Mesoporous Silica Thin Films as Robust Biocatalyst Platforms. *ACS Appl. Mater. Interfaces* **2010**, *2* (2), 360–365.
- (4) Rabe, M.; Verdes, D.; Seeger, S. Understanding Protein Adsorption Phenomena at Solid Surfaces. *Adv. Colloid Interface Sci.* **2011**, *162* (1–2), 87–106.
- (5) Gray, J. J. The Interaction of Proteins with Solid Surfaces. *Curr. Opin. Struct. Biol.* **2004**, *14* (1), 110–115.
- (6) Wei, T.; Carignano, M. A.; Szleifer, I. Molecular Dynamics Simulation of Lysozyme Adsorption/Desorption on Hydrophobic Surfaces. *J. Phys. Chem. B* **2012**, *116* (34), 10189–10194.
- (7) van der Veen, M.; Norde, W.; Stuart, M. C. Electrostatic Interactions in Protein Adsorption Probed by Comparing Lysozyme and Succinylated Lysozyme. *Colloids Surf. B Biointerfaces* **2004**, *35* (1), 33–40.
- (8) Meissner, J.; Prause, A.; Bharti, B.; Findenegg, G. H. Characterization of Protein Adsorption onto Silica Nanoparticles: Influence of PH and Ionic Strength. *Colloid Polym. Sci.* **2015**, *293* (11), 3381–3391.
- (9) Wittemann, A.; Ballauff, M. Interaction of Proteins with Linear Polyelectrolytes and Spherical Polyelectrolyte Brushes in Aqueous Solution. *Phys. Chem. Chem. Phys.* **2006**, *8* (45), 5269–5275.
- (10) Bremer, M. G.; Duval, J.; Norde, W.; Lyklema, J. Electrostatic Interactions between Immunoglobulin (IgG) Molecules and a Charged Sorbent. *Colloids Surf. Physicochem. Eng. Asp.* **2004**, *250* (1–3), 29–42.
- (11) Chen, K.; Xu, Y.; Rana, S.; Miranda, O. R.; Dubin, P. L.; Rotello, V. M.; Sun, L.; Guo, X. Electrostatic Selectivity in Protein–Nanoparticle Interactions. *Biomacromolecules* **2011**, *12* (7), 2552–2561.
- (12) Levin, A.; Czeslik, C. Interaction of Calmodulin with Poly(Acrylic Acid) Brushes: Effects of High Pressure, PH-Value and Ligand Binding. *Colloids Surf. B Biointerfaces* **2018**, *171*, 478–484.
- (13) Demanèche, S.; Chapel, J.-P.; Monrozier, L. J.; Quiquampoix, H. Dissimilar PH-Dependent Adsorption Features of Bovine Serum Albumin and α -Chymotrypsin on Mica Probed by AFM. *Colloids Surf. B Biointerfaces* **2009**, *70* (2), 226–231.
- (14) Höök, F.; Rodahl, M.; Kasemo, B.; Brzezinski, P. Structural Changes in Hemoglobin during Adsorption to Solid Surfaces: Effects of PH, Ionic Strength, and Ligand Binding. *Proc. Natl. Acad. Sci.* **1998**, *95* (21), 12271–12276.
- (15) Rosenfeldt, S.; Wittemann, A.; Ballauff, M.; Breininger, E.; Bolze, J.; Dingenouts, N. Interaction of Proteins with Spherical Polyelectrolyte Brushes in Solution as Studied by Small-Angle x-Ray Scattering. *Phys. Rev. E* **2004**, *70* (6), 061403.

- 1
2
3 (16) Henzler, K.; Haupt, B.; Lauterbach, K.; Wittemann, A.; Borisov, O.; Ballauff, M. Adsorption
4 of β -Lactoglobulin on Spherical Polyelectrolyte Brushes: Direct Proof of Counterion Release
5 by Isothermal Titration Calorimetry. *J. Am. Chem. Soc.* **2010**, *132* (9), 3159–3163.
- 6 (17) Galisteo, F.; Norde, W. Adsorption of Lysozyme and α -Lactalbumin on
7 Poly(Styrenesulphonate) Latices 1. Adsorption and Desorption Behaviour. *Colloids Surf. B*
8 *Biointerfaces* **1995**, *4* (6), 375–387.
- 9 (18) Biesheuvel, P. M.; van der Veen, M.; Norde, W. A Modified Poisson– Boltzmann Model
10 Including Charge Regulation for the Adsorption of Ionizable Polyelectrolytes to Charged
11 Interfaces, Applied to Lysozyme Adsorption on Silica. *J. Phys. Chem. B* **2005**, *109* (9),
12 4172–4180.
- 13 (19) Longo, G. S.; Szleifer, I. Adsorption and Protonation of Peptides and Proteins in PH
14 Responsive Gels. *J. Phys. Appl. Phys.* **2016**, *49* (32), 323001.
- 15 (20) Lund, M.; Åkesson, T.; Jönsson, B. Enhanced Protein Adsorption Due to Charge Regulation.
16 *Langmuir* **2005**, *21* (18), 8385–8388.
- 17 (21) Yigit, C.; Kanduč, M.; Ballauff, M.; Dzubiella, J. Interaction of Charged Patchy Protein
18 Models with Like-Charged Polyelectrolyte Brushes. *Langmuir* **2017**, *33* (1), 417–427.
- 19 (22) Peng, C.; Liu, J.; Zhao, D.; Zhou, J. Adsorption of Hydrophobin on Different Self-Assembled
20 Monolayers: The Role of the Hydrophobic Dipole and the Electric Dipole. *Langmuir* **2014**,
21 *30* (38), 11401–11411.
- 22 (23) Ninham, B. W.; Parsegian, A. Electrostatic Potential Between Surfaces Bearing Ionizable
23 Groups in Ionic Equilibrium with Physiological Saline Solution. *J. Theor. Biol.* **1971**, *31* (3),
24 405.
- 25 (24) Nap, R.; Gong, P.; Szleifer, I. Weak Polyelectrolytes Tethered to Surfaces: Effect of
26 Geometry, Acid-Base Equilibrium and Electrical Permittivity. *J. Polym. Sci. Part B Polym.*
27 *Phys.* **2006**, *44*, 2638–2662.
- 28 (25) Tagliacruzchi, M.; Calvo, E. J.; Szleifer, I. Molecular Theory of Chemically Modified
29 Electrodes by Redox Polyelectrolytes under Equilibrium Conditions: Comparison with
30 Experiment. *J Phys Chem C* **2008**, *112*, 458–471.
- 31 (26) Ricci, A. M.; Tagliacruzchi, M.; Calvo, E. J. Charge Regulation in Redox Active Monolayers
32 Embedded in Proton Exchanger Surfaces. *Phys. Chem. Chem. Phys.* **2012**, *14* (28), 9988.
- 33 (27) Tagliacruzchi, M.; Azzaroni, O.; Szleifer, I. Responsive Polymers End-Tethered in Solid-
34 State Nanochannels: When Nanoconfinement Really Matters. *J. Am. Chem. Soc.* **2010**, *132*
35 (35), 12404–12411.
- 36 (28) Stanton, C. L.; Houk, K. N. Benchmarking PKa Prediction Methods for Residues in Proteins.
37 *J. Chem. Theory Comput.* **2008**, *4* (6), 951–966.
- 38 (29) Bashford, D.; Karplus, M. Multiple-Site Titration Curves of Proteins: An Analysis of Exact
39 and Approximate Methods for Their Calculation. *J. Phys. Chem.* **1991**, *95* (23), 9556–9561.
- 40 (30) Tagliacruzchi, M.; Szleifer, I. Stimuli-Responsive Polymers Grafted to Nanopores and Other
41 Nano-Curved Surfaces: Structure, Chemical Equilibrium and Transport. *Soft Matter* **2012**, *8*
42 (28), 7292.
- 43 (31) Kubiak-Ossowska, K.; Jachimaska, B.; Mulheran, P. A. How Negatively Charged Proteins
44 Adsorb to Negatively Charged Surfaces: A Molecular Dynamics Study of BSA Adsorption
45 on Silica. *J. Phys. Chem. B* **2016**, *120* (40), 10463–10468.
- 46 (32) Hladílková, J.; Callisen, T. H.; Lund, M. Lateral Protein–Protein Interactions at Hydrophobic
47 and Charged Surfaces as a Function of PH and Salt Concentration. *J. Phys. Chem. B* **2016**,
48 *120* (13), 3303–3310.
- 49
50
51
52
53
54
55
56
57
58
59
60

- 1
2
3 (33) Swails, J. M.; Roitberg, A. E. Enhancing Conformation and Protonation State Sampling of
4 Hen Egg White Lysozyme Using PH Replica Exchange Molecular Dynamics. *J. Chem.*
5 *Theory Comput.* **2012**, *8* (11), 4393–4404.
- 6 (34) Li, L.; Li, C.; Sarkar, S.; Zhang, J.; Witham, S.; Zhang, Z.; Wang, L.; Smith, N.; Petukh, M.;
7 Alexov, E. DelPhi: A Comprehensive Suite for DelPhi Software and Associated Resources.
8 *BMC Biophys.* **2012**, *5* (1), 9.
- 9 (35) Vorobjev, Y. N.; Vila, J. A.; Scheraga, H. A. FAMBE-PH: A Fast and Accurate Method to
10 Compute the Total Solvation Free Energies of Proteins. *J Phys Chem B* **2008**, *112* (35),
11 11122–11136.
- 12 (36) Alexov, E. G.; Gunner, M. R. Incorporating Protein Conformational Flexibility into the
13 Calculation of PH-Dependent Protein Properties. *Biophys. J.* **72** (5), 2075–2093.
- 14 (37) Li, H.; Robertson, A. D.; Jensen, J. H. Very Fast Empirical Prediction and Rationalization of
15 Protein PKa Values. *Proteins* **2005**, *61* (4), 704–721.
- 16 (38) de Vos, W. M.; Leermakers, F. A. M.; de Keizer, A.; Cohen Stuart, M. A.; Kleijn, J. M. Field
17 Theoretical Analysis of Driving Forces for the Uptake of Proteins by Like-Charged
18 Polyelectrolyte Brushes: Effects of Charge Regulation and Patchiness. *Langmuir* **2010**, *26*
19 (1), 249–259.
- 20 (39) Fogolari, F.; Briggs, J. M. On the Variational Approach to Poisson–Boltzmann Free
21 Energies. *Chem. Phys. Lett.* **1997**, *281* (1–3), 135–139.
- 22 (40) Berisio, R.; Sica, F.; Lamzin, V.; Wilson, K.; Zagari, A.; Mazzarella, L. Atomic Resolution
23 Structures of Ribonuclease A at Six PH Values. *Acta Crystallogr. Sect. D* **2002**, *58* (3), 441–
24 450.
- 25 (41) Ramasubbu, N.; Paloth, V.; Luo, Y.; Brayer, G.; Levine, M. Structure of Human Salivary
26 A-amylase at 1.6 Å Resolution: Implications for Its Role in the Oral Cavity. *Acta*
27 *Crystallogr. Sect. D* **1996**, *52* (3), 435–446.
- 28 (42) Kontopidis George; Nordle Gilliver Anna; Sawyer Lindsay. Ovine B-lactoglobulin at Atomic
29 Resolution. *Acta Crystallogr. Sect. F* **2014**, *70* (11), 1498–1503.
- 30 (43) Basch, J. J.; Timasheff, S. N. Hydrogen Ion Equilibria of the Genetic Variants of Bovine β-
31 Lactoglobulin. *Arch. Biochem. Biophys.* **1967**, *118* (1), 37–47.
- 32 (44) Taulier, N.; Chalikian, T. V. Characterization of PH-Induced Transitions of β-Lactoglobulin:
33 Ultrasonic, Densimetric, and Spectroscopic Studies. *J. Mol. Biol.* **2001**, *314* (4), 873–889.
- 34 (45) Haynes, C. A.; Sliwinsky, E.; Norde, W. Structural and Electrostatic Properties of Globular
35 Proteins at a Polystyrene-Water Interface. *J. Colloid Interface Sci.* **1994**, *164* (2), 394–409.
- 36 (46) Tanford, C.; Hauenstein, J. D. Hydrogen Ion Equilibria of Ribonuclease1. *J. Am. Chem. Soc.*
37 **1956**, *78* (20), 5287–5291.
- 38 (47) Webb, H.; Tynan-Connolly, B. M.; Lee, G. M.; Farrell, D.; O’Meara, F.; Søndergaard, C. R.;
39 Teilum, K.; Hewage, C.; McIntosh, L. P.; Nielsen, J. E. Remeasuring HEWL PKa Values by
40 NMR Spectroscopy: Methods, Analysis, Accuracy, and Implications for Theoretical PKa
41 Calculations. *Proteins Struct. Funct. Bioinforma.* **2011**, *79* (3), 685–702.
- 42 (48) Lee, S. J.; Park, K. Protein Interaction with Surfaces: Separation Distance-dependent
43 Interaction Energies. *J. Vac. Sci. Technol. Vac. Surf. Films* **1994**, *12* (5), 2949–2955.
- 44 (49) Kubiak-Ossowska, K.; Cwieka, M.; Kaczynska, A.; Jachimska, B.; Mulheran, P. A.
45 Lysozyme Adsorption at a Silica Surface Using Simulation and Experiment: Effects of PH on
46 Protein Layer Structure. *Phys Chem Chem Phys* **2015**, *17* (37), 24070–24077.
- 47 (50) Kubiak-Ossowska, K.; Mulheran, P. A. Mechanism of Hen Egg White Lysozyme Adsorption
48 on a Charged Solid Surface. *Langmuir* **2010**, *26* (20), 15954–15965.
- 49
50
51
52
53
54
55
56
57
58
59
60

- 1
2
3 (51) Hildebrand, N.; Köppen, S.; Derr, L.; Li, K.; Koleini, M.; Rezwan, K.; Colombi Ciacchi, L.
4 Adsorption Orientation and Binding Motifs of Lysozyme and Chymotrypsin on Amorphous
5 Silica. *J. Phys. Chem. C* **2015**, *119* (13), 7295–7307.
6
7 (52) Yu, G.; Liu, J.; Zhou, J. Mesoscopic Coarse-Grained Simulations of Lysozyme Adsorption.
8 *J. Phys. Chem. B* **2014**, *118* (17), 4451–4460.
9
10 (53) Ellis, C. R.; Shen, J. PH-Dependent Population Shift Regulates BACE1 Activity and
11 Inhibition. *J. Am. Chem. Soc.* **2015**, *137* (30), 9543–9546.
12
13 (54) Clement, G. E.; Snyder, S. L.; Price, H.; Cartmell, R. The PH Dependence of the Pepsin-
14 Catalyzed Hydrolysis of Neutral Dipeptides. *J. Am. Chem. Soc.* **1968**, *90* (20), 5603–5610.
15
16 (55) Loewen, P. C.; Carpena, X.; Vidossich, P.; Fita, I.; Rovira, C. An Ionizable Active-Site
17 Tryptophan Imparts Catalase Activity to a Peroxidase Core. *J. Am. Chem. Soc.* **2014**, *136*
18 (20), 7249–7252.
19
20 (56) Gascón, V.; Márquez-Álvarez, C.; Blanco, R. M. Efficient Retention of Laccase by Non-
21 Covalent Immobilization on Amino-Functionalized Ordered Mesoporous Silica. *Appl. Catal.*
22 *Gen.* **2004**, *482*, 116–126.
23
24 (57) Francic, N.; Bellino, M. G.; Soler-Illia, G. J.; Lobnik, A. Mesoporous Titania Thin Films as
25 Efficient Enzyme Carriers for Paraoxon Determination/Detoxification: Effects of Enzyme
26 Binding and Pore Hierarchy on the Biocatalyst Activity and Reusability. *Analyst* **2014**, *139*
27 (12), 3127–3136.
28

29 TOC figure

